JOURNAL OF THE MECHANICAL BEHAVIOR OF BIOMEDICAL MATERIALS 37 (2014) 24–32

Available online at www.sciencedirect.com

ScienceDirect

www.elsevier.com/locate/jmbbm


Research Paper

# Multi-phonon scattering processes in one-dimensional anharmonic biological superlattices: Understanding the dissipation of mechanical waves in mineralized tissues

*Pierre-Yves Guerder*[a,d,*], *Alix C. Deymier-Black*[b], *Nichlas Z. Swinteck*[a], *Jérôme O. Vasseur*[c], *Olivier Bou-Matar*[d], *Krishna Muralidharan*[a], *Pierre A. Deymier*[a]

[a]*Department of Materials Science and Engineering, University of Arizona, Tucson, AZ 85721, USA*
[b]*Department of Orthopaedic Surgery, Washington University in St. Louis, St. Louis, MO 63110, USA*
[c]*Institut d'Electronique, de Microélectronique et de Nanotechnologie (IEMN, UMR CNRS 8520), PRES Lille Nord de France, 59652 Villeneuve d'Ascq, France*
[d]*International Associated Laboratory LEMAC: IEMN, UMR CNRS 8520, PRES Lille Nord de France, ECLille, 59652 Villeneuve d'Ascq, France*

ARTICLE INFO

*Article history:*
Received 8 January 2014
Received in revised form
28 April 2014
Accepted 3 May 2014
Available online 14 May 2014

*Keywords:*
Biological mineralized tissue
Mechanical energy dissipation
Multiphonon scattering
Hydroxyapatite/collagen
Superlattice

ABSTRACT

The scattering of elastic waves in a one dimensional phononic (PnC) crystal composed of alternate collagen and hydroxy-apatite constituent layers is studied. These superlattices are metaphors for mineralized tissues present in bones and teeth. The collagen is treated as an open system elastic medium with water content which can vary depending on the level of stress applied. The open system nature of the collagen–water system leads to a non-linear stress–strain response. The finite difference time domain method is employed to investigate the propagation of non-linear mechanical waves through the superlattice. The spectral energy density method enables the calculation of the non-linear vibrational wave band structure. The non-linearity in the mechanical response of the collagen–water system enables a variety of multi-phonon scattering processes resulting in an increase in the number of channels for the dissipation of elastic waves and therefore for the dissipation of mechanical energy. These results provide an explanation for the relationship between bone fragility and decreased hydration.



*Correspondence to: Materials Science and Engineering Department, The University of Arizona, 1235 E. James E. Rogers Way Room 141, P.O. Box 210012, Tucson, AZ 85721-0012, USA
*E-mail address:* pierre-yves.guerder@centraliens-lille.org (P.-Y. Guerder).

http://dx.doi.org/10.1016/j.jmbbm.2014.05.001
1751-6161/

## 1. Introduction

Mineralized biological tissues, such as bone and tooth, are hierarchical composite structures composed of a stiff hydroxyapatite (HAP) mineral phase, a compliant proteinaceous collagen phase, and water. At the nanoscale, bone and teeth are constituted of a periodic assembly of alternating regions of collagen and HAP in a hydrated environment with a repeat unit cell size of 67 nm (Ten Cate 1980). This periodic composite structure, forming a one dimensional (1-D) superlattice, is believed to be responsible for the remarkable strength and toughness of these biological materials (Jager and Fratzl 2000; Currey 2002; Deymier-Black et al. 2010). At the micrometer scale, mineralized tissues exhibit a large network of interconnected porosity, tubules in dentin and canaliculi and lacunae in bone, which allow for the transfer of nutrients, waste, and water throughout the tissue (Boyde and Lester 1967; Dillaman et al. 1991). This porosity allows bone and teeth to remain in equilibrium with water, maintaining hydration of the tissues. Water molecules exhibit a variety of different interactions with the HAP and collagen including the formation of water-bridges within the collagen helix, filling channels within the HAP, and surface hydration of the collagen and HAP phases (Bertinetti et al. 2007; De Simone et al. 2008; Ravikumar and Hwang 2008). Three-point bend and notch testing indicate that hydration has a significant impact on the mechanical properties of mineralized tissues resulting in increased elastic moduli as well as decreased toughness and loss of plastic behavior (Kahler et al. 2003; Kruzic et al. 2003; Nyman et al. 2006). Hydration increases the non-linear behavior of collagen as well as its elastic modulus while increasing its toughness (Grant et al. 2008; Gevorkian et al. 2013). It is theorized that these changes in the collagen mechanical behavior due to water content are the major cause for the changes in overall tissue mechanics. Although these tests provide important information about how hydration affects material properties, they provide no information about the dynamic properties of these tissues.

The number one cause of fracture in both bones and teeth is trauma or impact. To avoid fracture, the energy from sudden impacts must be dissipated in order to limit the formation of stress concentrators that can lead to tissue failure and fracture. It is therefore essential to understand how the composite structure of bone and teeth reacts to these dynamic loads which are so often responsible for fracture. In this study, it is theorized that the non-linear behavior of collagen in equilibrium with water provides a means of filling vibrational band gaps that arise from the periodicity of the HAP/collagen structure assembly. Under high load (high deformation) conditions, the non-linearity of the mechanical response of the collagen–water system may open up multiphonon scattering channels leading to a filling of the band gaps in the vibrational band structure of the HAP/collagen superlattice. We model the collagen/water system within the context of the thermodynamics of stressed open systems. This model leads to non-linear stress–strain relationships of the collagen. The non-linear model of the open collagen/water systems is incorporated into a dynamic model of the HAP/collagen superlattice. The propagation of elastic waves through that superlattice is investigated using the finite difference time domain (FDTD) method in conjunction with the spectral energy density (SED) method. Vibrational (phonon) wave band structures of the HAP/collagen/water system show that at high amplitudes, vibrational waves can interact with each other through multiphonon scattering channels that can fill the band gaps inherent in the band structure of elastic superlattices. This band-gap filling facilitates the propagation of vibrations in a larger range of frequencies, providing an effective mechanism for dissipation of mechanical energy, thus limiting the risk of failure.

This paper is organized as follows. In Section 2, we introduce the model of the open collagen/water system. This system is modeled within the context of the thermodynamics of stressed solid solutions. This model results in the formulation of the non-linear stress–strain response of the collagen/water solid, i.e. a strain dependent elastic modulus. Section 2 also presents the model of the HAP/collagen periodic structure in the form of a 1-D superlattice as well as the methods of FDTD and SED that are employed to investigate the dynamic response of the superlattice. In particular we focus on the calculation of the vibrational/phonon band structure of the superlattice as a function of the energy (amplitude) of the propagating elastic waves. In Section 3, we report the results of the calculations and provide an analysis of the effect of the non-linear elastic modulus. In particular, it is shown that high amplitude (energy) waves can interact with each other through multiple phonon scattering processes. These interactions lead to the opening of new channels for the dissipation of the elastic energy over a wider range of frequencies compared to the case of low energy waves.

Finally, conclusions are drawn in Section 4as to the relationship between the observed behavior and bone fragility due to decreased hydration.

## 2. Models and methods

### 2.1. Thermodynamics of stressed solid solution

To address the problem of the mechanical behavior of bone material in the presence of water, we develop the chemo-mechanical equations of states of materials that can adsorb fluids under stress based on the work of (Larche 1985; Larche and Cahn 1985). The total internal energy of the material is obtained as an integral of an internal Helmholtz energy density $f'$:

$$E = \int_{V'} f' \, dV' \tag{1}$$

where the energy density is given by

$$f' = f'(T, \varepsilon, ..., c_I', ...) \tag{2}$$

the prime indicates that all densities are relative to the reference state for measuring strain. $T$, $\varepsilon$, and $c_I'$ are the temperature, strain and molar density of chemical constituent "I", respectively. We consider $K$ variable the chemical species in the chosen materials. The differential form of Eq. (2) takes the form:

$$df'(T, \varepsilon_{ij}, c_I', ...) = s'(T, \varepsilon_{ij}, c_I', ...)\, ds' + \sigma_{ij}(T, \varepsilon_{ij}, c_I', ...)\, d\sigma_{ij} + \sum M_{I,K}(T, \varepsilon_{ij}, c_I', ...)\, dc_I' \tag{3}$$

the functions: $s'(T,\varepsilon_{ij},...,c_I',...)$, $\sigma_{ij}(T,\varepsilon_{ij},...c_I'...)$ and $M_{I,K}(T,\varepsilon_{ij},...c_I'...)$ are the density of entropy, stress and diffusion potential equations of state, respectively. The diffusion potential is used when considering a substitutional solid solution that constrains the molar densities according to: $c'_1+...+c'_I+...+c'_K=c'_0$ where $c'_0$ is the density of substitutional sites of the different chemical species. Introducing mole fractions $X_I=(c_I'/c_0')$ the diffusion potentials are therefore defined as:

$$\left(\frac{\partial f'}{\partial X_I}\right)_{T,\varepsilon,X_{I\neq K}}=c_0'M_{I,K}\quad\text{with}\quad I=1,\ K-1 \tag{4}$$

By choosing $K$ as a dependent chemical specie, one may treat the problem with only $K-1$, independent variables. Let us now simplify the problem to a binary solution i.e. $I=1$ and $K=2$. Note that the substitutional solid solution representation is equivalent to an interstitial solid solution if 1 represents the interstitial specie (e.g. water) and 2 the interstitial sites (i.e. available sites for water in a collagen matrix). Denoting by the composition in specie 1 by 'X' and using 2 as the dependent specie, the diffusion potential becomes:

$$M_{12}=\frac{1}{c_0'}\left(\frac{\partial f'}{\partial X_1}\right)_{T,\varepsilon} \tag{5}$$

It is convenient to define the free energy density $\Phi'$ by the Legendre transformation where strain is replaced by stress as variable.

$$\Phi'=f'-\sigma_{ij}\varepsilon_{ij} \tag{6}$$

The differential form of the density $\Phi'$ is

$$d\Phi'=-\varepsilon_{ij}\,d\sigma_{ij}-s'\,dT+c_0'M_{12}\,dX_1 \tag{7}$$

From this relation we deduce the following Maxwell relation:

$$-c_0'\left(\frac{\partial M_{12}}{\partial\sigma_{ij}}\right)_{T,X_1}=\left(\frac{\partial\varepsilon_{ij}}{\partial X_1}\right)_{T,\sigma_{kl}} \tag{8}$$

In the case of a binary solution whose elastic properties depend on the composition, the right hand side of Eq. (8) has to be written as:

$$\left(\frac{\partial\varepsilon_{ij}}{\partial X_1}\right)_{T,\sigma_{kl}}=\frac{\partial\varepsilon_{ij}^c}{\partial X_1}+\frac{\partial S_{ijkl}}{\partial X_1}\sigma_{kl} \tag{9}$$

where we have dropped the subscript in the differentials for the sake of simplifying the notation. $\varepsilon_{ij}^c$ is the component of the chemical strain and $S_{ijkl}$ is the component of the compliance tensor. The chemical strain is stress free and is only associated with the expansion or contraction of the material upon a change in composition. To simplify the notation, we take $\eta_{ij}=\partial\varepsilon_{ij}^c/\partial X_1$ where the linear coefficients $\eta_{ij}$ is the component of the chemical expansion coefficient tensor. The simplest relationship between the change in composition $(X-X_0)$ and the chemical strain is therefore:

$$\varepsilon_{ij}^c=(X-X_0)\eta_{ij}\delta_{ij} \tag{10}$$

$\delta_{ij}$ in Eq. (10) is the Kroenecker symbol. $X_0$ is the composition of the reference state for measuring strain. To obtain the second term in Eq. (9), we have used Hooke's law:

$$s_{ij}=C_{ijkl}(e_{kl}-e_{kl}^c) \tag{11}$$

or

$$\varepsilon_{ij}-\varepsilon_{ij}^c=S_{ijkl}\sigma_{kl} \tag{12}$$

$C_{ijkl}$ is the component of the stiffness tensor. The quantity $\varepsilon_{ij}^m=\varepsilon_{ij}-\varepsilon_{ij}^c$ is the mechanical strain.

Inserting Eq. (9) into Eq. (8) and after integration, the diffusion potential becomes:

$$c_0'M_{12}=-\frac{\partial\varepsilon_{ij}^c}{\partial X}\sigma_{ij}-\frac{1}{2}\frac{\partial S_{ijkl}}{\partial X}\sigma_{kl}\sigma_{ij}+\phi(X) \tag{13}$$

where $\varphi$ is some unknown function of composition. This unknown function is eliminated by choosing a hydrostatic state of pressure, P, as reference state. Inserting Eq. (10) into Eq. (13), the diffusion potential equation of state for the binary solution is now given as

$$M_{12}=\mu_1(T,P,X_2)-\mu_2(T,P,X_1)-V_0'\left[\eta_{ij}\sigma_{ij}-\eta_{kk}P-\frac{1}{2}\frac{\partial S_{ijkl}}{\partial X_1}\sigma_{kl}\sigma_{ij}+\frac{1}{2}P^2\frac{\partial S_{ijkl}}{\partial X_1}\delta_{kl}\delta_{ij}\right] \tag{14}$$

where $V_0'=1/c_0'$.

In Eq. (14), we have introduced the chemical potentials of species 1 and 2. Under hydrostatic pressure, the diffusion potential is nothing but a difference in chemical potential. The chemical potentials are defined as: $\mu_i(T,P,X_i)=(1/c'_0)(\partial f'/\partial X_I)_{T,\varepsilon,X_{j\neq i}}$.

The condition for chemical equilibrium of the binary solid solution in contact with a binary fluid solution is determined by the conservation of the diffusion potential:

$$\begin{aligned}&M_{12}(\sigma,x)=\mu_1-\mu_2\\&\mu_1^F=\mu_1\\&\mu_2^F=\mu_2\end{aligned} \tag{15}$$

We now make the temperature dependency implicit and drop $T$ from the equations.

Subtracting the diffusion potentials of a stress solid solution, $M_{12}$ and a solid solution under hydrostatic pressure, $\overline{M}_{12}$ yields:

$$M_{12}-\overline{M}_{12}=\mu_1^F-\overline{\mu}_1^F-(\mu_2^F-\overline{\mu}_2^F) \tag{16}$$

$\overline{\mu}_2^F\mu_1^F$, $\overline{\mu}_1^F$, and $\mu_2^F$ are the chemical potentials of species 1 and 2 in the fluid when the solid is subjected to a stress or to a hydrostatic pressure only, provided that the fluid behaves like a chemical reservoir; this is the case if we consider the fluid to be a reservoir of water only; the difference on the right hand side of Eq. (16) becomes identically equal to 0 and the diffusion potentials of the stressed and unstressed systems are equal. Note that the diffusion potential of the stressed solid is evaluated at the composition $X$ while the hydrostatic diffusion potential is the difference in chemical potential of species 1 and 2 at equilibrium hydrostatic composition $X^0$. The diffusion potential of the stressed system can be calculated from

$$M_{12}=\mu_1(P,X_1^0)-\mu_2(P,X_2^0) \tag{17}$$

Eq. (17) is sufficient to solve the change in composition, $X-X^0$, of the solid to maintain equilibrium under stress with the fluid reservoir. For this, we use the equation of state (14).

$$\mu_1(T,P,X_1^0)-\mu_2(T,P,X_2^0=1-X_1^0)=\mu_1(T,P,X_1)-\mu_2(T,P,X_2=1-X_1)-V_0'\left[\eta_{ij}\sigma_{ij}-\eta_{kk}P-\frac{1}{2}\frac{\partial S_{ijkl}}{\partial X_1}\sigma_{kl}\sigma_{ij}+\frac{1}{2}P^2\frac{\partial S_{ijkl}}{\partial X_1}\delta_{kl}\delta_{ij}\right] \tag{18}$$

It is clear that Eq. (18) leads to a composition which is a non-linear function of stress. Then, inserted into equation of states (10) and (12), the stress–strain relation becomes non-linear.

To simplify the problem, we assume that the collagen–water binary obeys the prototypical regular solution model. The molar free energy of mixing:

$$f_m = RT(X_1 \ln X_1 + (1-X_1)\ln(1-X_1)) + \Omega(1-X_1)X_1 \quad (19)$$

$\Omega$ represents the interaction energy between species 1 (water) and 2 (water sites in collagen). In this case the difference in chemical potential is given by

$$\mu_1(T,P,X_1) - \mu_2(T,P,X_2 = 1-X_1) = RT \ln \frac{X_1}{1-X_1} + \Omega(1-2X_1) \quad (20)$$

We now assume that the equilibrium mole fraction of water in collagen in the absence of stress is $X_1^0 = 0.5$. Molecular dynamics simulations of the interaction between collagen and water indicate that the occupancy of water sites, both internal and external to the collagen helix, is approximately 40–60% (De Simone et al. 2008; Ravikumar and Hwang 2008). Under this condition, in the absence of stress, the difference of chemical potential given by Eq. (20) is zero. We further assume that the elastic coefficients of collagen are independent of water content. This is justified based on the fact that the speed of sound and the density of polymer-based media and water are very similar. Finally, reducing the problem to a 1-D one, we rewrite Eq. (20) in the form:

$$RT \ln \frac{X_1}{1-X_1} + \Omega(1-2X_1) = V_0' \eta \sigma \quad (21)$$

To obtain Eq. (21) we have also neglected the hydrostatic pressure $P$ compared to the stress. The chemo-mechanical problem of a collagen solid matrix in equilibrium with a water reservoir then can be solved by eliminating composition between Eq. (21) and Eq. (22):

$$\varepsilon = \frac{1}{Y}\sigma + \eta(X_1 - X_1^0) \quad (22)$$

Eq. (22) is the 1-D version of Eq. (12) combined with Eq. (10). There $Y$ is Young's modulus of collagen with the stress free water content, $X_1^0 = 0.5$.

Bowman et al. (1996) have measured the stress versus strain relationship in demineralized bovine bone under uniaxial tension and open conditions (i.e. in equilibrium with water). The non-linear stress–strain curve for tensile stress is extracted from Bowman et al. The part of the curve for the negative values of the strain is the symmetrical of the positive part, as it is in the equations above. Fig. 1 shows a fit to this data obtained by eliminating composition between Eqs. (21) and (22). We found that the best fit is achieved for the following conditions: $\eta = 0.12$, $Y = 7.75 \times 10^8$ Pa, $\Omega = 5448.9$ J/mole and $V'_0 = 4.56 \times 10^{-4}$ m$^3$/mole. These values are in agreement with values of $\eta = 0.09$ and $Y = 0.5$–1 GPa, measured for type 1 collagen (Catanese Iii et al. 1999; Heim and Matthews 2006; Fullerton et al. 2011).

Eqs. (21) and (22) which describe the open-system stress–strain relationship by elimination of the compositional variable $X$, include five parameters. After fitting the model to the available experimental stress–strain curve, one obtains three of the parameters that are in excellent agreement with

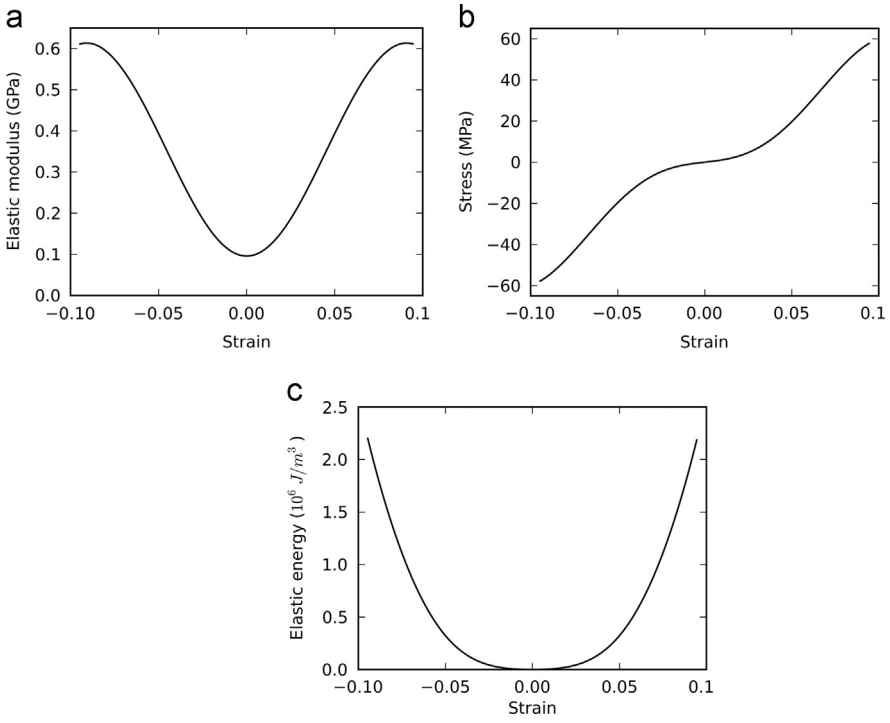


**Fig. 1 – (a) Young's modulus versus strain for open collagen/water system. The curve is a Taylor expansion up to order 8 that fits the experimental data. (b) Stress versus strain for collagen in the presence of water. This is obtained by multiplying Young's modulus by the strain: $\sigma = Y(\varepsilon)\varepsilon$. (c) Energy versus strain for collagen in the presence of water. The curve is obtained by integrating the stress versus strain curve.**

published data for collagen. The other two parameters take on values that are physically meaningful.

From the fit, Young's modulus $Y(\varepsilon)$ and the elastic energy $E(\varepsilon)$ are written as Taylor series up to the 8th order.

$$Y(\varepsilon) = a_0 + a_2\varepsilon^2 + a_4\varepsilon^4 + a_6\varepsilon^6 + a_8\varepsilon^8 \tag{23}$$

and

$$E(\varepsilon) = \frac{a_0}{2}\varepsilon^2 + \frac{a_2}{4}\varepsilon^4 + \frac{a_4}{6}\varepsilon^6 + \frac{a_6}{8}\varepsilon^8 \tag{24}$$

with $a_0 = 9.565 \times 10^7$ Pa, $a_2 = 1.543 \times 10^{11}$ Pa, $a_4 = -1.571 \times 10^{13}$ Pa, $a_6 = 6.958 \times 10^{14}$ Pa and $a_8 = -1.650 \times 10^{16}$ Pa.

Young's modulus, stress and elastic energy versus the strain obtained with this Taylor series are represented in Fig. 1.

### 2.2. 1-D model and spectral energy density-finite difference time domain (SED-FDTD) method

We now consider the 1-D model illustrated in Fig. 2 as representative of the nanoscale, periodic assembly of alternating regions of collagen and HAP in bone and teeth. The finite superlattice is composed of $N = 2560$ masses of materials A and B connected by non-linear springs. Material A is chemically inert and represents HAP. Material B represents the open collagen/water system i.e. collagen that can adsorb water from a reservoir. The behavior of elastic modes in this model is simulated using a modified Spectral Energy Density-Finite Difference Time Domain (SED-FDTD) method. The SED-FDTD method has been used recently with success to simulate the propagation of elastic wave propagation in phononic crystals (Thomas et al. 2010). In its original version, this method solves the springs and masses equation by discretizing time and space (x-axis) and by replacing derivatives by finite differences. We extend this approach to include chemo-mechanical effects by using the non-linear stress-strain relation described in Section 2.1 (Eq. 23). The non-linear spring constant depends on the water content in accordance with the non-linear stress–strain relation of the collagen/water open system. Owing to the 1-D nature of the system, we assume that lateral diffusion of water into material B (collagen) is much faster than the acoustic wave and that material B is always at equilibrium with respect to chemical composition. Under this condition, the 1-D mass-spring equation is given by

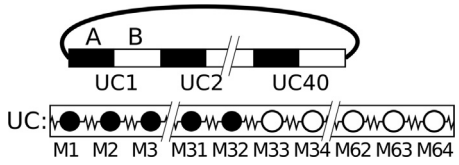


**Fig. 2 – Schematic representation of the simulated HAP/collagen 1-D periodic system. The unit cells (UC) are heterogeneous media composed 32 masses of a material A mimicking HAP that does not change composition when subjected to stress and 32 masses of material B. B is a collagen collagen-based material that can interact with a chemical reservoir of water it is embedded into. Each mass is connected to its two neighbors by two springs. A spring is linear (respectively nonlinear) if the mass on its left is composed of material A (resp. material B). Periodic boundary conditions are imposed at the end of the system, which contains 40 UCs.**

$$m_i \frac{\partial^2 u_i}{\partial t^2} = f_i + f_{i-1} \quad \text{with} \quad m_i = \rho_i \times \Delta x^3 \tag{25}$$

where $t$ is time, $\rho_i$ is the mass density, $u(t)$ is the displacement. The displacement is related to the mechanical strain by $\varepsilon = (\partial u/\partial x)$ and $\sigma$ is the stress. $\Delta x$ is the distance between two adjacent masses. In 1-D, we describe the stress–strain relation by

$$\sigma = Y(\varepsilon)\varepsilon \tag{26}$$

or the force-displacement relation by

$$f_i = k_i\, du_i = \rho_i c_{L,i}^2 \Delta x\, du_i \quad \text{with} \quad k_i = \rho_i c_{L,i}^2 \Delta x \quad \text{and} \quad c_{L,i} = \frac{Y(\varepsilon)_i}{\rho_i} \tag{27}$$

Eq. (25) is solved discretely and takes the form:

$$\rho_i \Delta x^3 \frac{\partial^2 u_i}{\partial t^2} = \left[\rho_i c_{L,i}^2 (u_{i+1} - u_i) - \rho_{i-1} c_{L,i-1}^2 (u_i - u_{i-1})\right] \Delta x \tag{28}$$

In Eq. (28) we assume that the mass density is independent of composition. This is the case in material A. Since the mass density of water and collagen are similar, the mass densities of discrete points in material B are also taken to be constant.

The structure is composed of 40 unit cells each of them composed of 64 masses (32 of them composing the material A and the 32 others composing the material B). Each mass is connected to its two neighbors by two springs. A spring is linear (respectively nonlinear) if the mass on its left is composed of material A (resp. material B). The nonlinear spring constant is calculated using Eq. (27) where $Y(\varepsilon)$ is the Taylor expansion of Young's modulus described in Section 2.1.

The distance between the two adjacent masses $\Delta x = 1.04$ nm. The time integration step, $\Delta t$, is given by $\Delta t = \Delta x/(40c^{(A)}) = 6 \times 10^{-15}$ s where $c^{(A)}$ is the speed of sound in the medium A. The total number of time steps used in our calculations is $2^{22}$ time steps. Periodic boundary conditions are applied at the free ends of the homogeneous regions to simulate an infinite superlattice. The thickness of the segments of material A and B are designated by $L_A$ and $L_B$. For the sake of simplicity we take $L_A = L_B = 33.5$ nm. Hence the length of a unit cell is $a = 67$ nm, the repeat unit cell size of mineralized collagen.

We use the SED-FDTD method to calculate the presence of acoustic modes in the crystal for different wave vectors. In particular, the SED method enables the projection of the vibrations of a structure onto a set of plane waves characterized by a wave vector (wave number in 1D) and a frequency. With this method, an initial random displacement is applied to each of the 2560 masses which imparts an initial potential energy to the structure. Then, the system is free to evolve during the total number of time steps ($2^{22}$) and the speed of each mass is recorded during the last $2^{21}$ time steps. For each mass, this speed is projected on a considered wave number and a Fourier transform provides the frequency distribution of the energy in the solid. This energy is averaged over the 64 masses of each unit cell. This operation is repeated 200 times for which the results are averaged, in order to allow a sufficient

variety of initial energy distribution. The SED-FDTD method is a way of knowing how often a phononic mode is visited.

The dimension chosen for the system, 40 unit cells, allows the whole operation to be repeated over 21 wave numbers ranging from 0 to $\pi/a$ by step of $0.05\pi/a$. The values used for the initial displacement of the masses are $\Delta x/45$ and $\Delta x/150$. The wave number interval $[0, \pi/a]$ constitute the first Brillouin zone of the phononic periodic structure.

We compare the time resolution of our calculation with the diffusion time for water in collagen. If we approximate the 1-D system by a wire with a l=0.5 nm cross section, and if we consider a diffusion coefficient for water in collagen of $D = 2.5 \times 10^{-5}$ cm$^2$/s (Westover and Dresden 1974), the time for diffusion through the wire is on the order of $t = l^2/(6D) = 1.67 \times 10^{-11}$ s. If we compare this time to the maximum frequency that we study, namely 20 GHz, we obtain a characteristic time of $5 \times 10^{-11}$ s. This time is significantly larger than the time for diffusion through the model system.

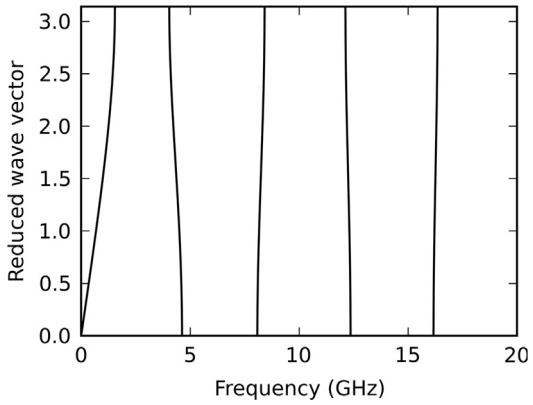


**Fig. 3 – Band structure of the AB superlattice. The wave vector is expressed in reduced units of 1/$a$ where $a$ is the period of the HAP/collagen superlattice. The band structure is determined from Eq. (29).**

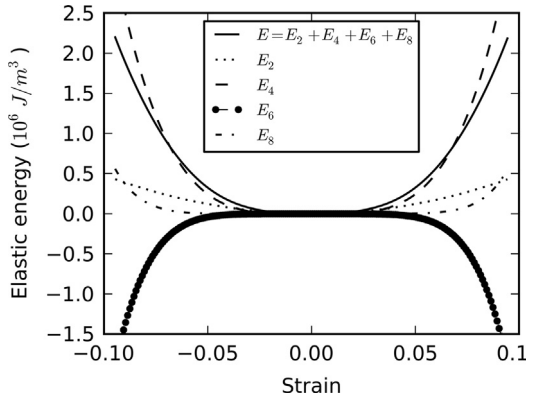


**Fig. 4 – Elastic energy versus strain for the collagen/water open system. The solid line is the same as that in Fig. 1, namely the integral of the Taylor series decomposition of the stress as a function of strain. The dotted and dashed lines are the terms of orders 2, 4, 6 and 8 of this Taylor series. The term of order 6 is particularly interesting as it is gives a concave down curve characteristic of an unstable system (its second derivative is negative).**

So, even at high frequencies, we can assume that water content of the system is at equilibrium at all times. This assumption is even more valid when considering low frequency modes.

As for the convergence of the method, the SED-FDTD calculation was performed using 16, 32 and 64 masses per unit cell in the limit of small displacements. We observed that the band diagram obtained with 16 masses per unit cell almost matched the linear results below 10 GHz but not above this frequency. The band diagram obtained with 64 masses per unit cell matched almost perfectly the linear band diagram as shown in Fig. 4a. The band diagram obtained with 32 masses per unit cell was an intermediary result, with a match better than that for 16 but worse than that for 64 masses per unit cell. Hence, the value of 64 masses per unit cell was chosen for all the SED-FDTD calculations.

## 3. Results

### 3.1. Analytical results

The model structure of our mineralized biological tissue is a superlattice with the period $a = L_A + L_B = 67$ nm. The elastic band structure of an infinite AB superlattice can be calculated analytically by (Camley et al. 1983)

$$\cos(ka) = Ch_A Ch_B + \frac{1}{2}\left(\frac{F_A}{F_B} + \frac{F_B}{F_A}\right) Sh_A Sh_B \tag{29}$$

where

$$Ch_I = \cosh(\alpha_I L_I),$$
$$Sh_I = \sinh(\alpha_I L_I)$$
$$F_I = \alpha_I C^{(I)} \quad \text{and} \quad I = A, B.$$
$$\alpha_I^2 = k_{//}^2 - \rho^{(I)} \frac{\omega^2}{C^{(I)}}$$

For a 1-D superlattice, the component of the wave vector perpendicular to the x-direction is zero, i.e. $k_{//} = 0$ and the hyperbolic functions in Eq. (29) reduce to trigonometric functions.

The elastic band structure of the AB superlattice with fixed water content of B, $X_1^0 = 0.5$, can be calculated readily and is illustrated in Fig. 3. This is the band structure of the elastic superlattice, that is, when the collagen/water system keeps a constant composition and its corresponding Young's modulus remains constant. In this case, the superlattice exhibits elastic passing bands separated by wide band gaps. Elastic waves will propagate through the HAP/collagen superlattice only when their frequency will fall into the range of the passing bands. Waves with frequency in the band gap will not propagate and will be only reflected by the superlattice.

### 3.2. Numerical results

The spectral energy density of the structure for an initial displacement of $\Delta x/150$ (low amplitude) is provided in Fig. 5a and that for an initial displacement of $\Delta x/45$ (large amplitude) is provided in Fig. 5b. At low amplitude, the spectrum shows very thin peaks at specific frequencies corresponding to the vibrational modes that are found when the transmission is solved analytically (Fig. 3). The system behaves according to

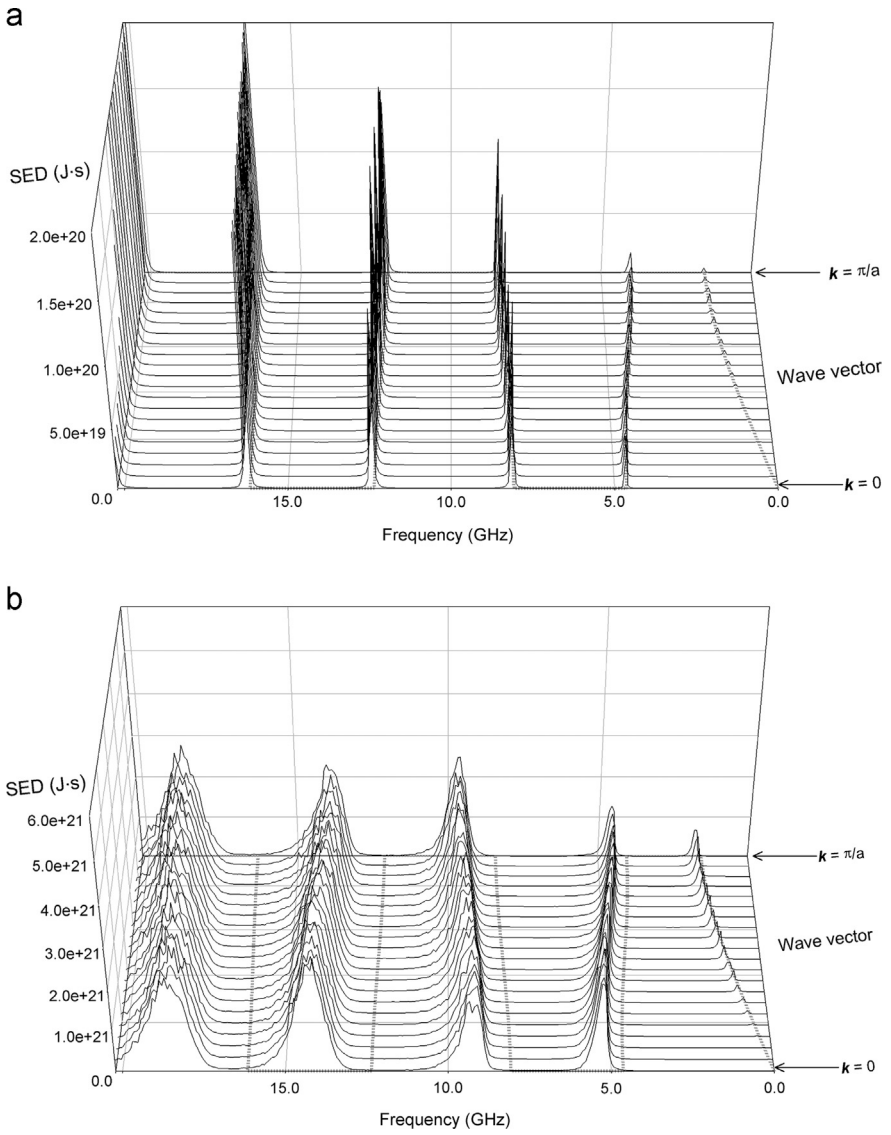


**Fig. 5 – Solid black lines: spectral energy density of the phononic crystal structure with an initial displacement of (a) $\Delta x/150$ and (b) $\Delta x/45$. Gray dashes: linear band structure of the superlattice shown in Fig. 3.**

linear elasticity; it shows a harmonic behavior. In this regime, the elastic coefficient (Young's modulus) of the collagen (B) region retains its value at a small strain. For all the frequency range (0–20 GHz), an excellent agreement between this non-linear result and the linear result obtained with Eq. (29) is observed.

At a large amplitude, the system becomes strongly non-linear. The peaks broaden significantly. A filling of the band gaps is observed, as shown in Fig. 6. This band gap filling is more visible at higher frequencies (10–20 GHz), which allows us to think that as frequency increases, the band gaps will be more and more filled. At higher frequencies (hundreds of GHz), this would mean that the energy is dissipated as thermal phonons.

The peak broadening and frequency shift are interpreted as follows. If we limit Young's modulus function of strain to its constant term, which is exactly the linear case, then the Taylor series expansion of the elastic energy function is limited to its second order term, which appears in Fig. 4. In that case, the spectrum from the SED-FDTD calculation only contains the "primary" frequencies which are that of a linear system. This result is shown in Fig. 6.

Now, if we limit Young's modulus function of strain to its terms up to order 2, the energy function contains a term of order 2 and a term of order 4. As shown in Fig. 6, the system simulated in the SED-FDTD program behaves as a non-linear system with the frequency shift and band gap filling described above.

If we limit Young's modulus function to its terms up to order 4 (resp. 6), the energy function contains terms of order 2, 4 and 6 (resp. 2, 4, 6, 8). Taking those terms into account (see Fig. 6) does not change the behavior of the system, which proves that the second order term of Young's modulus (fourth order term of the energy) plays the major role for the nonlinear behavior and the terms of higher order do not play a significant role. Hence, we can assert that this nonlinear behavior associated with a fourth-order function in strain elastic energy is mainly due to four-wave (four-phonon)

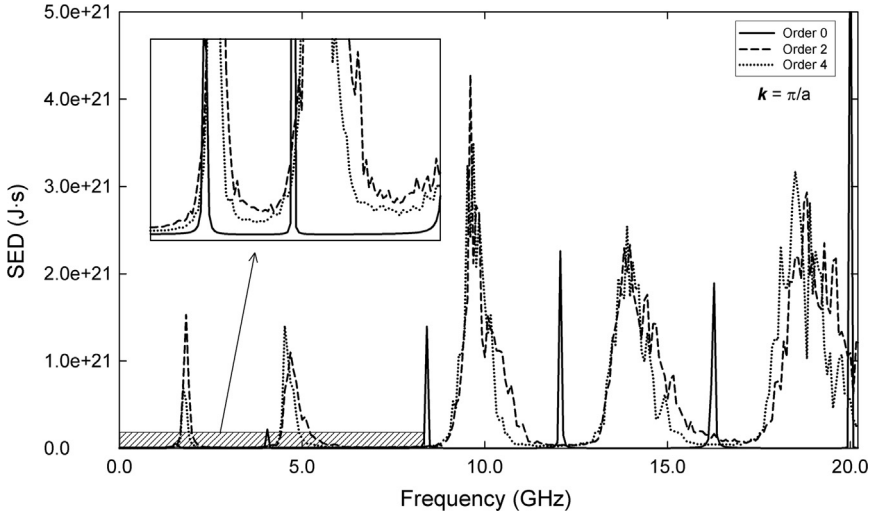


**Fig. 6 – Spectral energy density (SED) of the phononic crystal structure with an initial displacement of $\Delta x/45$ for wave vector $\pi/a$. Gray solid line: with Young's modulus truncated at the order zero (constant value, linear case); dashes: with Young's modulus truncated at the order 2; and dots: with Young's modulus truncated at the order 4. Curves with Young's modulus truncated at orders 6 and 8 are not included since they do not carry significant changes compared to order 4. Inset: magnified highlight of the band gap filling in the frequency range between 0 and 8 GHz.**

interactions. Indeed, considering that the dynamic strain is a linear superposition of plane waves with different wave numbers and frequencies and raising this superposition to the fourth power to estimate the energy, leads to four-wave interactions. These scattering interactions would conserve momentum and frequency and may involve a variety of processes such as the splitting of a single phonon into three others, the scattering of two phonons forming two others, etc. (Manktelow et al. 2011; Swinteck et al. 2013). Those new phonons interactions offer more channels for the dispersion of mechanical energy.

We can relate the behavior of our non-linear superlattice to the behavior of a multiple-well mass-spring system. A multiple-well system is a system for which the representation of the elastic energy as a function of strain is not parabolic but is a superposition of infinity of parabolas. To each parabola corresponds a single value of the spring constant. Hence, representing a non-quadratic energy map by a multiplicity of parabolic wells is equivalent to introducing a continuum of values of spring constants. At high amplitudes, waves will sample wider ranges of strain values, effectively visiting the multiplicity of energy wells. The band diagram will show a continuity of modes above the "primary" frequencies of the linear system. Those bands broaden and finally fill the gaps. The passing bands of this system will also be shifted to higher frequencies.

In our case, the reason why the spring constants increase as a function of the magnitude of the strain is that the model we chose for Young's modulus is symmetrical and has only even orders in its Taylor series expansion. If an asymmetrical function was used for Young's modulus, its Taylor series expansion would contain odd order terms. In that case, nonlinear modes with frequencies less than the "primary" frequencies would appear. We would also observe a shift of the passing bands to lower frequencies.

## 4. Conclusions

A 1-D phononic crystal composed of a superlattice of alternate collagen and hydroxy-apatite constituent layers is studied. This serves as a model of mineralized biological tissue. The collagen layers are treated as an open system that can absorb or desorb water. This collagen/water open system results in a non-linear Young's modulus. This open system model is fitted to experimental data. We study the dynamic response of the non-linear superlattice to the propagation of elastic waves. A FDTD method coupled to a SED calculation is performed to obtain the wave band structure. In the linear limit, the band structure is composed of passing bands separated by band gaps that forbid the propagation of elastic waves over some ranges of frequency. The non-linearity of the collagen layers in the superlattice gives rise to multi-wave (phonon) scattering processes that lead to partial band gap filling. Multi-phonon scattering processes constitute ways of opening new channels for the dissipation of mechanical energy. This mechanism for mechanical energy dissipation is the direct consequence of the hydration of the collagen.

The risk of dentin and bone fracture has been shown to increase with age. During aging, there is also a marked decrease in the level of interconnected porosity in both tissues (Kinney et al., 2005; Weinstein et al. 2010). This filling of the porosity is associated with decreased fluid flow and therefore decreased hydration of the tissues. It has previously been theorized that this decrease in hydration may in part be responsible for the increased fragility of bone and dentin with age; however, the associated mechanism remained unclear (Manolagas 2010). The results presented here provide a possible explanation for the relationship between bone fragility and decreased hydration. The presence of interstitial

water in the collagen phase increases its plastic behavior, but more importantly allows it to act non-linearly. When mineralized tissues undergo a traumatic event, the non-linearity of the collagen allows for band gap filling, thus allowing a larger range of frequencies to propagate mechanical waves through the material. This ease of propagation diminishes the formation of stress concentrations by vibrational modes that would otherwise be banned from propagation, reducing the risk of fracture. In turn, a decrease in hydration will lead the collagen to act more linearly, which is done here by limiting Young's modulus to its constant term, and as a result limit the number of channels that can dissipate elastic energy and frequencies which are allowed to propagate, thus increasing the development of stress concentrations and the possibility of fracture.

## Acknowledgments

We acknowledge partial support from the Centre National de la Recherche Scientifique (CNRS) through Laboratoire International Associé (LIA) "MATEO" between the University of Arizona and the Institut d'Electronique, de Microélectronique et de Nanotechnologie.

The first author acknowledges support from the Bourse Mobilité Recherche from Conseil Régional du Nord Pas-de-Calais (France).

## REFERENCES

Bertinetti, L., Tampieri, A., Landi, E., Ducatti, C., Midgley, P.A., Coluccia, S., Martra, G., 2007. Surface structure, hydration, and cationic sites of nanohydroxyapatite: UHR-TEM, IR, and microgravimetric studies. J. Phys. Chem. C 111, 4027–4035.

Bowman, S.M., Zeind, J., Gibson, L.J., Hayes, W.C., McMahon, T.A., 1996. The tensile behavior of demineralized bovine cortical bone. J. Biomech. 29, 1497–1501.

Boyde, A., Lester, K.S., 1967. An electron microscope study of fractured dentinal surfaces. Calcif. Tissue Res. 1, 122–136.

Camley, R.E., Djafarirouhani, B., Dobrzynski, L., Maradudin, A.A., 1983. Transverse elastic-waves in periodically layered infinite and semi-infinite media. Phys. Rev. B 27, 7318–7329.

Catanese Iii, J., Iverson, E.P., Ng, R.K., Keaveny, T.M., 1999. Heterogeneity of the mechanical properties of demineralized bone. J. Biomech. 32, 1365–1369.

Currey, J.D., 2002. In: Bones: Structure and Mechanics. Princeton University Press, Princeton, NJ.

De Simone, A., Vitagliano, L., Berisio, R., 2008. Role sn. Biochem. Biophys. Res. Commun. 372, 121–125.

Deymier-Black, A.C., Almer, J.D., Stock, S.R., Haeffner, D.R., Dunand, D.C., 2010. Synchrotron X-ray diffraction study of load partitioning during elastic deformation of bovine dentin. Acta Biomater. 6, 2172–2180.

Dillaman, R.M., Roer, R.D., Gay, D.M., 1991. Fluid movement in bone: theoretical and empirical. J Biomech. 1, 163–177.

Fullerton, G.D., Amurao, M., Rahal, A., Cameron, I.L., 2011. Micro-Ct dilatometry measures of molecular collagen hydration using bovine extensor tendon. Med. Phys. 38, 363–376.

Gevorkian, S.G., Allahverdyan, A.E., Gevorgyan, D.S., Simonian, A. L., Hu, C.K., 2013. Stabilization and anomalous hydration of collagen fibril under heating. PLoS One 8, 0078526.

Grant, C.A., Brockwell, D.J., Radford, S.E., Thomson, N.H., 2008. Effects of hydration on the mechanical response of individual collagen fibrils. Appl. Phys. Lett. 92, 233902.

Heim, A.J., Matthews, W.G., 2006. Determination of the elastic modulus of native collagen fibrils via radial indentation. Appl. Phys. Lett. 89, 181902.

Jager, I., Fratzl, P., 2000. Mineralized collagen fibrils: a mechanical model with a staggered arrangement of mineral particles. Biophys. J. 79, 1737–1746.

Kahler, B., Swain, M.V., Moule, A., 2003. Fracture-toughening mechanisms responsible for differences in work to fracture of hydrated and dehydrated dentine. J. Biomech. 36, 229–237.

Kinney, J.H., Nalla, R.K., Pople, J.A., Breunig, T.M., Ritchie, R.O., 2005. Age-related transparent root dentin: mineral concentrations, crystallite size and mechanical properties. Biomaterials 26, 3363–3376.

Kruzic, J.J., Nalla, R.K., Kinney, J.H., Ritchie, R.O., 2003. Crack blunting, crack bridging and resistance-curve fracture mechanics in dentin: effect of hydration. Biomaterials 24, 5209–5221.

Larche, F.C., 1985. Thermodynamics of stressed solids. Am. Ceram. Soc. Bull. 64 (1344-1344).

Larche, F.C., Cahn, J.W., 1985. The interactions of composition and stress in crystalline solids. Acta Metall. 33, 331–357.

Manktelow, K., Leamy, M., Ruzzene, M., 2011. Multiple scales analysis of wave–wave interactions in a cubically nonlinear monoatomic chain. Nonlinear Dyn. 63, 193–203.

Manolagas, S.C., 2010. From estrogen-centric to aging and oxidative stress: a revised perspective of the pathogenesis of osteoporosis. Endocr. Rev. 31, 266–300.

Nyman, J.S., Roy, A., Shen, X., Acuna, R.L., Tyler, J.H., Wang, X., 2006. The influence of water removal on the strength and toughness of cortical bone. J. Biomech. 39, 931–938.

Ravikumar, K.M., Hwang, W., 2008. Region-specific role of water in collagen unwinding and assembly. Proteins 72, 1320–1332.

Swinteck, N.Z., Muralidharan, K., Deymier, P.A., 2013. Phonon scattering in one-dimensional anharmonic crystals and superlattices: analytical and numerical study. J. Vib. Acoust. 135 (041016-041016).

Ten Cate, A.R., 1980. Oral Histology: Development, Structure and Function. Mosby, St Louis, MO.

Thomas, J.A., Turney, J.E., Iutzi, R.M., Amon, C.H., McGaughey, A.J. H., 2010. Predicting phonon dispersion relations and lifetimes from the spectral energy density. Phys. Rev. B. 81, 081411.

Weinstein, R.S., Wan, C., Liu, Q., Wang, Y., Almeida, M., O'Brien, C. A., Thostenson, J., Roberson, P.K., Boskey, A.L., Clemens, T.L., Manolagas, S.C., 2010. Endogenous glucocorticoids decrease skeletal angiogenesis, vascularity, hydration, and strength in aged mice. Aging Cell 9, 147–161.

Westover, C.J., Dresden, M.H., 1974. Collagen hydration: pulsed nuclear magnetic resonance studies of structural transitions. Biochim. et Biophys. Acta (BBA) - Protein Struct. 365, 389–399.